

Numerical study on the initiation of oblique detonation waves in a stoichiometric hydrogen-air mixture

Tao Wang, ^{a)} Yining Zhang, ^{b)} Honghui Teng, ^{a)} Zonglin Jiang ^{a)} and Hoi Dick Ng ^{c)}

a) State Key Laboratory of High Temperature Gas Dynamics, Institute of Mechanics, Chinese Academy of Sciences, Beijing, 100190, China;

b) State Key Laboratory of Laser Propulsion & Application, Beijing Power Machinery Research Institute, Beijing, 100074, China;

c) Department of Mechanical and Industrial Engineering, Concordia University, Montreal, QC H3G 1M8, Canada

Abstract

Two-dimensional oblique detonations induced by a wedge are simulated using the reactive Euler equations with a detailed chemical reaction model. The focus of this study is on the oblique shock-to-detonation transition in a stoichiometric hydrogen-air mixture. A combustible gas mixture at low pressure and high temperature, corresponding to the realistic inflow conditions applied in Oblique Detonation Wave Engines (ODWE), is presented in this study. At practical flight conditions, the present numerical results illustrate that the oblique detonation initiation is achieved through a smooth transition from the oblique arc shock, which differs from the abrupt transition depicted in previous studies. The formation mechanism of this smooth transition is discussed, and a quantitative analysis is carried out by defining a characteristic length for the initiation process. The dependence of the initiation length on different parameters including the wedge angle, flight Mach number and inflow Mach number is discussed.

I. Introduction

In recent years, high efficiency propulsion systems have generated great interest for their use in the development of air-breathing hypersonic aircrafts. The concept of oblique detonation waves has led to the development of Oblique Detonation Wave Engines (ODWE) [1] and Ram Accelerators [2]. This class of propulsion systems not only has the advantages of the Scramjet (Supersonic combustion ramjet), but also achieves a high thermal cycle efficiency through the detonation mode of combustion [3]. However, it remains technically challenging to establish the steady oblique detonations in high-speed combustible mixtures for propulsion applications, and such success requires more fundamental understanding of the oblique detonation structure and instability.

Early research conducted on oblique detonation waves was usually simplified into an oblique shock wave with a post-shock energy release zone attached to the wedge [4,5]. With the use of shock polars, the coupling relation of the oblique shock and combustion are discussed and analyzed [6,7,8]. Nevertheless, studies demonstrate that the realistic structure near the wedge front tip is rather complex. Li et al. [9] simulated numerically the oblique detonation, and observed the structure composed of a nonreactive oblique shock, an induction region, a set of deflagration waves, and the oblique detonation surface. This structure is verified experimentally [10] and considered as the standard structure used widely in many subsequent studies. Based on this structure, Sislian et al. [11,12] studied the near Chapman–Jouguet oblique detonation waves and propulsive performance of oblique detonation engines. Papalexandris [13] and Choi et al. [14] observed the fine scale structures characterized with “saw tooth” flame on oblique detonation surfaces, whose formation is

attributed to the instability of the coupling between the oblique shock and chemical reaction. Although the formation of triple points would be suppressed by high degrees of overdrive, the recent studies by Teng et al. [15,16] show that oblique detonation surfaces are unconditionally unstable, and the dynamics is similar to that of multi-dimensional cellular detonations. Small scale instability features are observed on the oblique detonation surface, similar to the unstable frontal structure of a normal cellular detonation [16,17,18]. Moreover, oblique detonation waves induced by the conical [19,20] and spherical projectiles [21,22] are investigated in the literature, depicting similar structures.

It is worth noting that previous studies mainly focus on the instability of oblique detonation surfaces, however the oblique shock-to-detonation transition does not yet attract enough attention. Studies suggest that both abrupt and smooth transition structures exist [23,24]. The abrupt structure is achieved by a multi-wave point connecting the oblique shock and the detonation surface; while the smooth one originates from an arc shock instead of the multi-wave point. Teng and Jiang [25] analyzed the structural differences of these two transition processes as a function of different chemical and aerodynamic parameters, and the criteria on the transition type are then proposed. Furthermore, the observed transient structures are also depend on the inflow Mach number toward the wedge and chemical activation energy [26,27], making the modeling of realistic oblique detonations more complex.

Transition from oblique shock to detonation is the origin of successful oblique detonation initiation; consequently its research is crucial in the design of ODWE. Recent studies [28,29,30] on the normal detonation initiation have demonstrated that both the aerodynamic

and mixture thermodynamic properties greatly influence the initiation of detonation. However, a deep knowledge of the oblique structure found in ODWE is still lacking and must be fully addressed. For simplicity, most of the previous studies [5-9,13-20] use simplified chemical reaction models, mainly one-step irreversible Arrhenius kinetic model. In addition, the inflow parameters are usually set artificially, deviating far from those in actual ODWE applications. To address the aforementioned issues, oblique detonation waves in a stoichiometric hydrogen-air mixture are investigated in this study with detailed chemistry. The inflow parameters are chosen to simulate the flow conditions in ODWE at high altitude. The numerical results will illustrate that the initiation of oblique detonation waves at these practical flow conditions is achieved by a smooth shock-to-detonation transition. The mechanism of ODW formation from the smooth transition is also studied, and the effect of the flight Mach number, inflow Mach number and wedge angle is analyzed quantitatively by defining a characteristic length scale for the initiation process.

II. Mathematical model and computational details

A schematic of an ODWE [31] and the wedge-induced oblique detonation is shown in Fig. 1. M_0 denotes the flight number of the aircraft and M_1 is the inflow Mach number of the combustible gas mixture inducing the oblique detonation wave from the wedge. One simplification used in this study is that the fuel mixing in supersonic flow is not considered. In other words, this study assumes the inflow to be well-premixed and focuses primarily on the resulting oblique detonation structure. Considering a flight altitude of 30 km and Mach number of 10, the flow is first pre-compressed twice by weak oblique shock waves in the

inlet diffuser. The combustible inflow then reflects on the two-dimensional wedge and first generates an oblique shock wave. The shock wave may trigger exothermic chemical reactions, and subsequently induce an oblique detonation wave downstream. For the present numerical study, the computational domain is bounded by the dashed zone shown in Fig. 1, whose coordinates are rotated to the direction along the wedge surface.

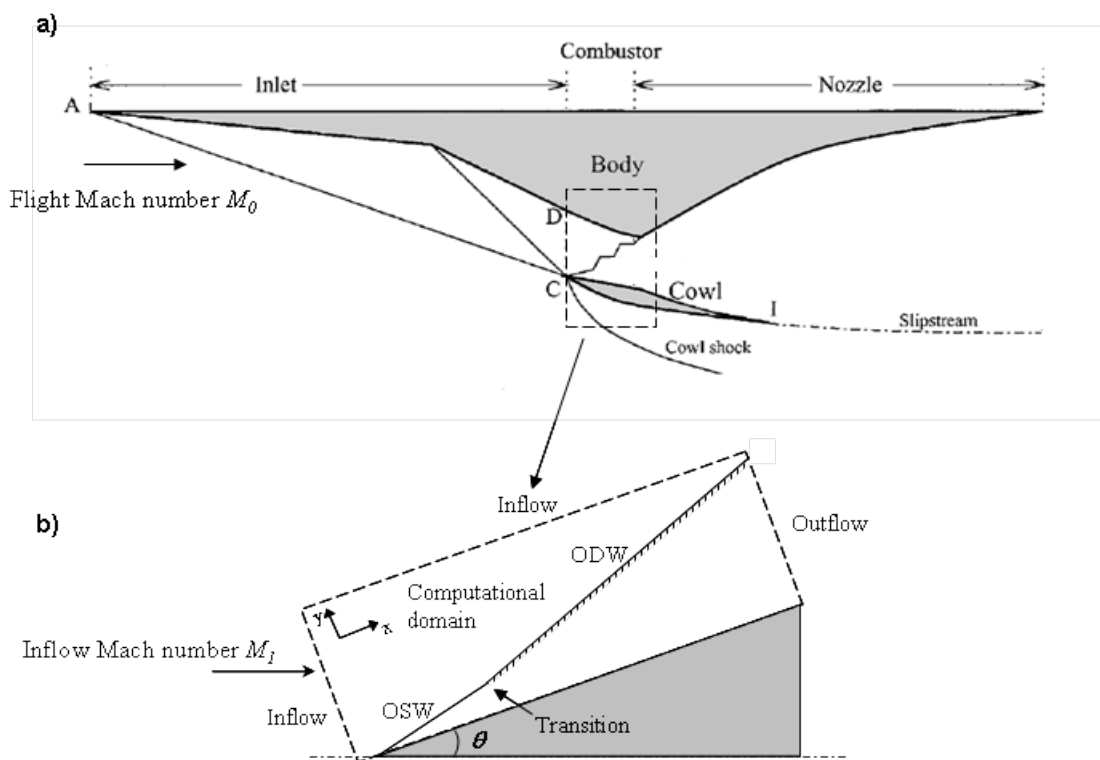


Figure 1. Schematic of a) an ODWE [31] and b) the wedge-induced oblique detonation from an inflowing combustible gas mixture

Previous results [23,32] demonstrated that the viscosity has negligible effects on the ODW structure. In keeping with previous simulations an inviscid assumption is also invoked in this work, as a result the boundary layer effect is not included in this study. Governing equations are thus simplified as the two-dimensional multi-species Euler equations written as

follows:

$$\frac{\partial \mathbf{U}}{\partial t} + \frac{\partial \mathbf{F}}{\partial x} + \frac{\partial \mathbf{G}}{\partial y} = \mathbf{S} \quad (1)$$

where:

$$\mathbf{U} = \begin{Bmatrix} \rho_1 \\ \vdots \\ \rho_n \\ \rho u \\ \rho v \\ e \end{Bmatrix}, \quad \mathbf{F} = \begin{Bmatrix} \rho_1 u \\ \vdots \\ \rho_n u \\ \rho u^2 + p \\ \rho uv \\ (e + p)u \end{Bmatrix}, \quad \mathbf{G} = \begin{Bmatrix} \rho_1 v \\ \vdots \\ \rho_n v \\ \rho uv \\ \rho v^2 + p \\ (e + p)v \end{Bmatrix}, \quad \mathbf{S} = \begin{Bmatrix} \omega_1 \\ \vdots \\ \omega_n \\ 0 \\ 0 \\ 0 \end{Bmatrix} \quad (2)$$

In the above equations, the total density and total energy are calculated by:

$$\rho = \sum_{i=1}^n \rho_i, \quad e = \rho h - p + \frac{1}{2} \rho (u^2 + v^2) \quad (3)$$

where specific enthalpy can be written as $h = \sum_{i=1}^n \rho_i h_i / \rho$ with h_i obtained from thermodynamic database of each individual species. Equation of state is

$$p = \sum_{i=1}^n \rho_i \frac{R_0}{w_i} T \quad (4)$$

where w_i is the molecular weight and T is the gas temperature; ω_i is the species specific mass production rate, which is decided by the chemical reaction model. The governing equations are then solved on adaptive unstructured quadrilateral grids [33] using the MUSCL-Hancock scheme [34]. This numerical scheme approaches the second-order accuracy in space and time by constructing the Riemann problem on the inter-cell boundary through the equations:

$$\begin{aligned} \bar{U}_i^L &= U_i^L + \frac{\Delta t}{2\Delta x} [F(U_i^L) - F(U_i^R)] \\ \bar{U}_i^R &= U_i^R + \frac{\Delta t}{2\Delta x} [F(U_i^L) - F(U_i^R)] \end{aligned} \quad (5)$$

The solution of the associated Riemann problem is computed by the HLLC approximate Riemann solver. Hydrogen/air chemical reaction model [35] is selected from the widely used CHEMKIN package and the mechanism consists of 11 species (H_2 , O_2 , O , H , OH , HO_2 , H_2O_2 ,

H₂O, N₂, N, NO) and 23 elementary reactions. The CHEMKIN database of thermodynamic parameters was used without modification. The stiff nature of the problem due to the chemical reaction calculation is solved by the DVODE package [36]. Stoichiometric hydrogen-air mixture with H₂:O₂:N₂ = 2:1:3.76 is used. The slip reflecting boundary condition is used on the wedge surface and the other boundaries are interpolated under the assumption of the zero first-order derivatives of all flow parameters. Unless specified, the computational domain of 60 mm × 20 mm is used and initially covered by a primary mesh of 0.2mm × 0.2mm. Adaptive mesh refinement (AMR) is based on the density gradient [33], the highest numerical resolution contains the finest grid size of 0.025 mm with three levels of refinement. The wedge begins at $x = 1.0$ and the length scale is in mm for all figures shown in subsequent sections.

III. Numerical results and discussion

To simulate the flow dynamics in an ODWE, the flight conditions need to be prescribed to determine the inflow pressure and temperature. Air-breathing aircrafts equipped with an ODWE are typically designed to operate at high altitude about 25-35 km and can cover a range of Mach numbers. Considering a flight altitude of 30 km and a flight Mach number M_o of 10, the ambient flow is pre-conditioned twice by weak oblique shock waves in the aircraft inlet. The implicit relation between the oblique shock angle β and deflection angle ϕ is given by:

$$\tan^3 \beta + A \tan^2 \beta + B \tan \beta + C = 0 \quad (6)$$

where

$$\begin{aligned}
A &= \frac{1 - M^2}{\tan \phi [1 + (\gamma - 1)M^2 / 2]} \\
B &= \frac{1 + (\gamma + 1)M^2 / 2}{1 + (\gamma - 1)M^2 / 2} \\
C &= \frac{1}{\tan \phi [1 + (\gamma - 1)M^2 / 2]}
\end{aligned} \tag{7}$$

Using the above equations, the oblique shock angle β can be calculated. The latter can then be used to determine the inflow pressure and temperature. Considering a typical deflection angle $\phi = 12.5^\circ$ and a resulting inflow Mach number $M_1 = 4.3$, a static pressure approximately 56 kPa and static temperature 1021 K are obtained. In this study, the wedge angle θ inducing the oblique detonation varies between 11° - 20° . The flight Mach number M_o and altitude have complex effects on pre-detonation inflow parameters. The flow is first simplified in this computational study such that the inflow Mach number M_1 varies between 4.0 and 5.0 without considering the change of static pressure and temperature. Afterward, the effects of inflow pressure and temperature, associated with the variation of flight Mach number M_o , are simulated and discussed.

3.1 Structures of oblique detonation waves

The oblique detonation structure resulting from an inflow Mach number M_1 of 4.3 and wedge angle of 15° is shown in Fig. 2. Notably it can be observed that this structure is different from the abrupt transition considered in most of the previous studies. The transition is smooth with an arc shock, and there is no obvious contact surface in the combustion product. In order to verify the effect of numerical grid resolution on such observations, detonation simulations with different grid sizes are carried out using the same initial and mixture conditions. Figure 3 compares the flow field of pressure with different grid sizes. The upper portion is simulated

with the finest grid of 0.0125 mm and the lower one with the finest grid of 0.025 mm. It can be observed that the difference is negligible, and the resolution with the finest grid 0.025 mm is therefore considered sufficient to study this problem. Furthermore, using the grid size of 0.025 mm gives about 10 grids in the half reaction zone along the streamline behind the corresponding overdriven detonation. The same effective grid resolution is also used in recent studies [15,16], which demonstrate that both the structure and instability of oblique detonation surfaces can be correctly captured with this resolution. The oblique detonation structure given in both Fig. 2 and Fig. 3 depict the smooth transition, which is different from the widely-studied abrupt transition. It is worth noting again that oblique shock and detonation surfaces are connected by a multi-wave turning point in the abrupt transition, while surfaces in the smooth transition are connected by an arc shock.

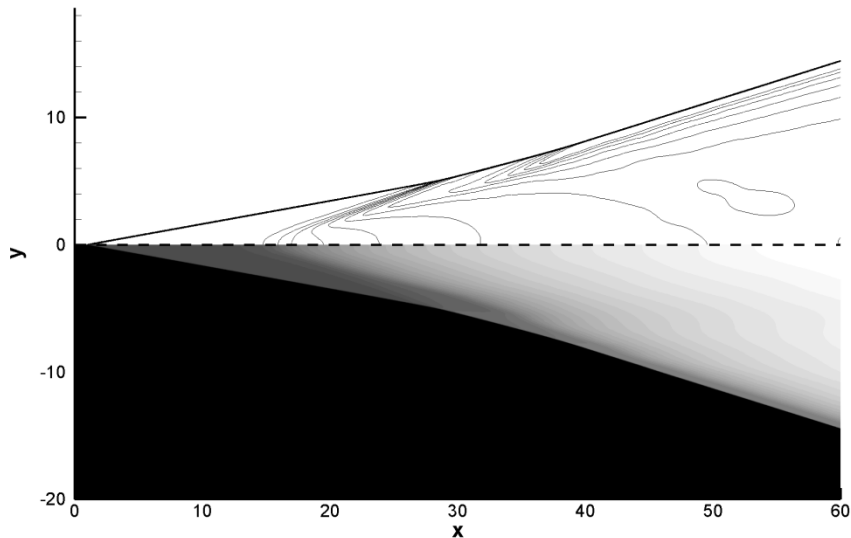


Figure 2. Pressure (upper) and temperature (lower) fields in the case of an inflow Mach number M_1 of 4.3 and wedge angle of 15°

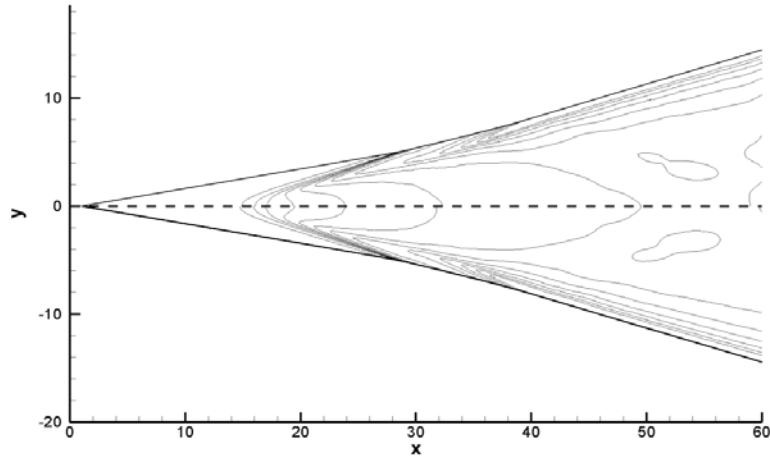


Figure 3. Resolution study of the oblique detonation structure in the case of an inflow Mach number M_1 of 4.3 and wedge angle of 15°

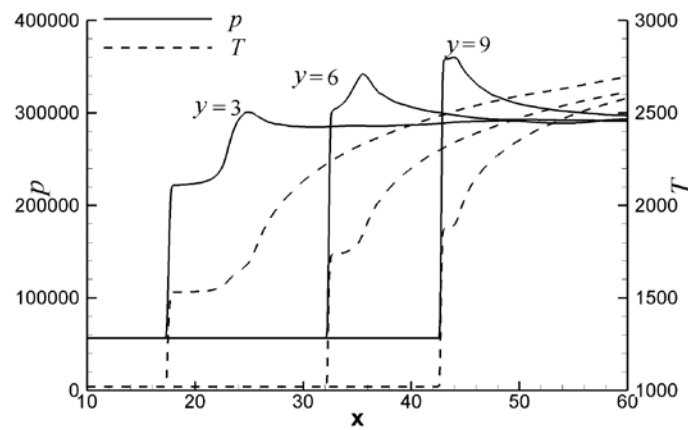


Figure 4. Pressure and temperature along the line paralleled with the x -axis in the case of an inflow Mach number M_1 of 4.3 and wedge angle of 15°

Figure 4 represents the pressure and temperature along different lines paralleled with the x -axis, demonstrating different combustion characteristics in this structure. Along the line $y = 3$, a long induction zone can be seen where there is about 10-mm separation between the shock and pressure peak induced by the heat release. Along the line $y = 6$, the oblique shock increases the pressure and temperature higher than those along the line $y = 3$. This results in a shorter induction zone, and the heat release is intensified. The line $y = 9$ corresponds to the

oblique detonation surface, demonstrating the fully coupled structure between the oblique shock and the chemical reaction. It can be observed that the pressure and temperature along the line $y = 6$ are different from those of a fully-established oblique detonation. This region can be viewed as an intermediate structure during the smooth transition of the oblique shock to oblique detonation.

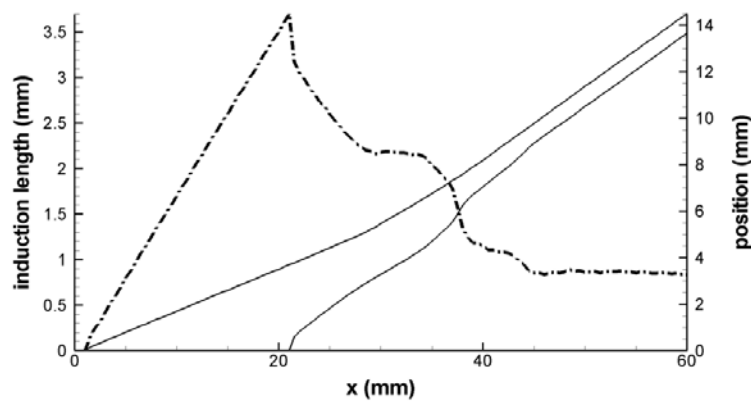


Figure 5. Induction zone length in the case of an inflow Mach number M_1 of 4.3 and wedge angle of 15°

To analyze the coupling relation between the oblique shock and subsequent heat release, Fig. 5 shows the induction zone length in the case of an inflow Mach number M_1 of 4.3 and wedge angle of 15° . Given the same combustible mixture with the same detailed chemical reaction mechanism, the steady Zel’dovich-von Neumann-Döring (ZND) structure of the corresponding Chapman-Jouguet (CJ) detonation can be computed with the CHEMKIN package [35]. The latter indicates that the temperature at the end of the ZND induction zone is about 2070 K. This critical temperature is chosen here to denote roughly the end of the induction zone in this study. The positions of the oblique shock and the end of the induction zone, along the line parallel with the y -axis, are shown through the right ordinate in Fig. 5.

The induction zone length is deduced and shown through left ordinate in Fig. 5, representing the projection of real reaction zone length on the vertical direction. Using this approach, the disturbance of reaction zone can be magnified considerably.

It can be seen that the induction zone length increases first since there is no chemical heat release until about $x = 20$. The chemical reactions begin and subsequently induce the deflagration, resulting in a decrease of the induction zone. The length appears to decrease rapidly at first, but soon a plateau is established between $x = 30$ to $x = 35$. This plateau corresponds to the intermediate structure of the smooth transition, which is quasi-steady. The induction zone length decreases further, and reaches its final stage gradually at about $x = 45$. It is worth noting that this length variation is quite different from that of the abrupt transition observed in the previous study [15]. In those cases, the induction zone length decreases drastically without the plateau, to a minimum value near the multi-wave point. Then a re-increasing trend can be observed so the length will reach the final value. However, there appears a quasi-steady plateau in this smooth transition, demonstrating the weak coupling of shock and heat release during this process. Similarly, this resembles the quasi-detonation in rough tubes [37], and this plateau can perhaps be viewed as the quasi-steady structure in oblique detonation phenomena.

These aforementioned results are consistent with the previous study on the formation mechanism of different ODW structures [25]. The oblique detonation angle is bigger than the oblique shock angle due to the heat release. Previous study [25] suggests that the abrupt transition appears if the angle difference is large, while the smooth transition appears if the angle difference is small. The critical value found in [25] is approximately 16° . The oblique

detonation angle β_{det} can be calculated by:

$$\frac{\tan\beta_{\text{det}}}{\tan(\beta_{\text{det}} - \theta)} = \frac{(\gamma + 1)M^2 \sin^2 \beta_{\text{det}}}{\gamma M^2 \sin^2 \beta_{\text{det}} + 1 - \sqrt{(M^2 \sin^2 \beta_{\text{det}} - 1)^2 - 2(\gamma^2 - 1)M^2 \sin^2 \beta_{\text{det}} Q}} \quad (8)$$

If the heat release $Q = 0$, the oblique detonation angle becomes the oblique shock angle. In this study, the combustible gas mixture deduced from the ODWE flight conditions has high temperature and low pressure. Hence, the density of the inflow mixture is rather low, and the heat release is limited. This implies that the difference of oblique shock and detonation angle is small, leading toward the smooth transition in ODWE. Indeed, the angle difference for all cases in the present study lies between 5° and 10° .

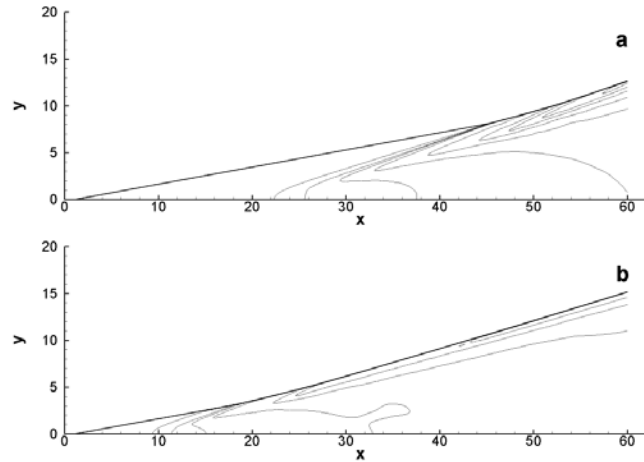


Figure 6 Pressure field in the cases of an inflow Mach number M_1 of 4.3 and wedge angle of 13° (a) and 17° (b)

3.2 Effects of wedge angle and inflow Mach number M_1

Oblique detonation structures in ODWE are influenced by several factors. In this study, the effects of two key parameters, namely, the wedge angle inducing the ODW and the inflow Mach number M_1 are further investigated. To study the effects of wedge angles, two more

cases with $\theta = 13^\circ$ and 17° are simulated and results are shown in Fig. 6. Notably, the initiation position moves downstream when the wedge angle decreases, and vice-versa. For instance, for increasing values of wedge angles 13° , 15° to 17° , the corresponding initiation positions are approximately $x = 45$, 30 , 20 mm, respectively. Structures in the cases of different inflow Mach numbers are shown in Fig. 7, with the same wedge angle 15° . It is found that the initiation position of both cases locate closely at $x = 30$ mm. Although the difference can be observed, the variation of the initiation position is not as significant as the change caused by the wedge angle.

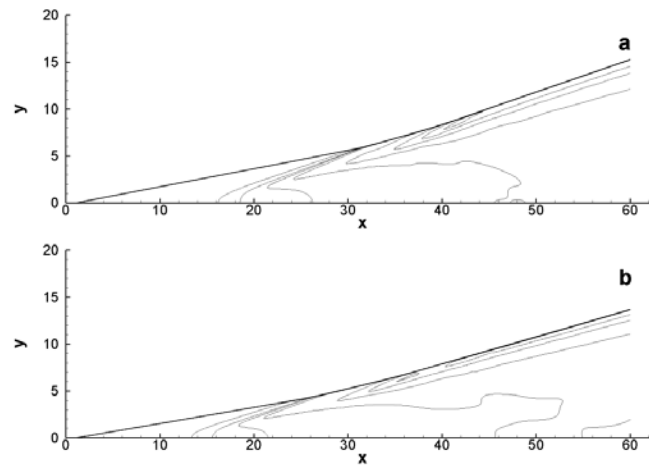


Figure 7 Pressure field in the cases of a wedge angle 15° , and inflow Mach number M_1 of 4.1 (a) and 4.5 (b)

Generally, numerical results show that the initiation position is insensitive to the inflow Mach number M_1 , but sensitive to the wedge angle θ . The initiation process is rather complex and significantly influenced by post-shock thermodynamic parameters and wave dynamics [27]. However, one can notice that in these cases the inflow gas mixtures have indeed reached a sufficiently high temperature close to the auto-ignition limit before interacting with the wedge, so initiation can be viewed as shock-accelerating ignition. To this end, initiation is

strongly dependent on temperature or sensitive to the oblique shock strength. A wedge angle of 15° , produces a post-oblique-shock temperature of approximately 1510K and 1577K whereby the inflow Mach number $M_1 = 4.1$ and 4.5. On the other hand, with an inflow Mach number of 4.3, post-oblique-shock temperature is 1455K and 1640K in the cases of wedge angle 13° and 17° , respectively. Consequently the wedge angle has a larger influence on the initiation position.

In order to further enhance the quantitative analysis, it is useful to define a characteristic length scale for the initiation process. An initiation length, along the flow stream direction paralleled with the x -axis, is considered in this study. It starts from the oblique shock and terminates at the end of induction zone, corresponding to the temperature value of 2070 K. Note that the lengths are different dependent on their distances from the wedge, and thus for convenience the characteristic length of initiation is given by the maximum one of each case which locates on the wedge surface.

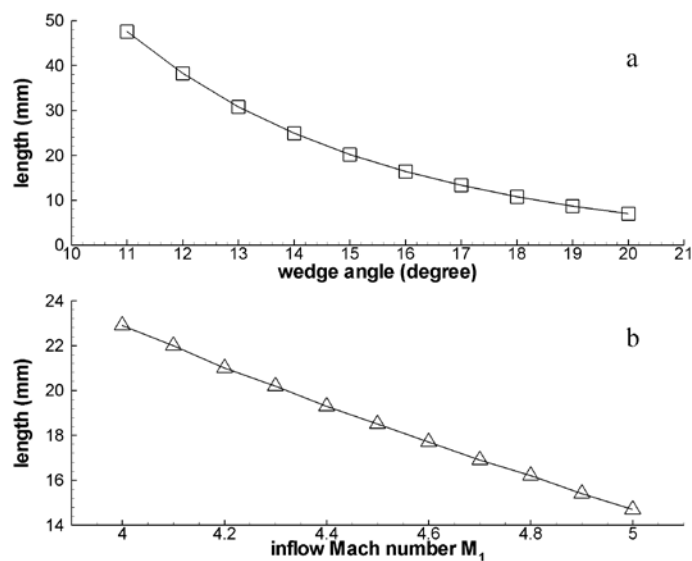


Figure 8. Characteristic length as a function of the wedge angle with an inflow Mach number M_1 of 4.3 (a), and as a function of the inflow Mach number M_1 with a wedge angle of 15° (b)

Figure 8 shows the characteristic length as a function of the wedge angle and inflow Mach number M_1 . When $M_1 = 4.3$, the length decreases when the wedge angle increases as shown in Fig. 8(a). Similar relations between the length and M_1 can be observed in Fig. 8(b), with a wedge angle of 15° . However, it can be observed that the length dependence on the wedge angle and inflow Mach number M_1 is quite different. The length varies nonlinearly with the wedge angle, while the variation between the length and M_1 is almost linear. This suggests that M_1 itself can only vary in a narrow range, compared with the wedge angle. However, varying M_1 is different from wedge angle because the former is limited by the flight condition, but the latter can be chosen freely as an adjusting parameter to establish the oblique detonation. Larger intervals of wedge angle produce longer ranges of characteristic length, revealing the nonlinear dependence as shown in Fig. 8(b).

From the pressure field (e.g. Fig. 2), the coupling between pressure waves and combustion is apparent in close proximity below the oblique shock. Near the wedge, the mixture is completely burned and there is only weak pressure build-up and the formation of pressure waves. According to this observation, the characteristic initiation length can be approximated theoretically based on post-oblique-shock conditions, which are available from classic aerodynamic theory. In addition, the theoretical result is based on the constant volume combustion calculation using the CHEMIKIN package [35]. First the post-oblique-shock specie densities and temperature are used to simulate the constant volume combustion and to obtain the combustion time corresponding to the mixture temperature of 2070 K. The theoretical initiation length is then calculated by multiplying the time with the post-oblique-shock velocity. Despite its simple formulation, this theoretical analysis may

provide a predictive approach for the general structure of oblique detonations. Table 1 shows the comparison of numerical and theoretical initiation length, together with the percentage difference between the two results. It is found that the theoretical length is smaller than the corresponding numerical one. In the cases listed in Table 1, error increases monotonously from 21.0% to 28.8% with increasing wedge angle. Differences between the numerical and theoretical results are mainly from the constant volume assumption in the theoretical analysis. Also, in the case of high angle, the error becomes large due to the stronger gasdynamic effect. Despite the magnitude of the error, it is a good step for a more quantitative study on oblique detonations. It is important to note that previous studies [27,38] on the initiation region demonstrate a rather complicated process, sometimes unpredictable, whose length depends on the balance of several factors. Although the method suggested in this study for the length prediction remains qualitative, it provides a simple first-step analysis moving forward from the totally unpredicted regime.

Table 1. Comparison of numerical and theoretical initiation length

| Angle | Numerical | Theoretical | Error |
|--------------|------------------|--------------------|--------------|
| 11 | 47.6 | 38.40 | 21.0% |
| 12 | 38.3 | 30.85 | 21.5% |
| 13 | 30.8 | 24.94 | 21.6% |
| 14 | 24.9 | 20.02 | 22.7% |
| 15 | 20.2 | 16.28 | 23.2% |
| 16 | 16.4 | 13.18 | 24.2% |
| 17 | 13.3 | 10.72 | 25.1% |
| 18 | 10.8 | 8.68 | 26.5% |
| 19 | 8.7 | 7.04 | 27.5% |
| 20 | 7.0 | 5.69 | 28.8% |

3.3 Effects of flight Mach number M_o

In order to study the effects of flight Mach number M_o , two more cases are simulated. The flight altitude remains 30 km, but the flight Mach number M_o changes to 8 and 9. Also the ambient flow is again compressed twice by weak oblique shock waves, with a deflection angle of 12.5° . Table 2 shows the corresponding static pressure, temperature and inflow Mach number M_1 for each of these additional cases.

Table 2 Static pressure, temperature and inflow Mach number M_1 in the cases of different flight Mach number M_o

| Flight Mach number M_o | P [kPa] | T [K] | Inflow Mach number M_1 |
|--------------------------|-----------|---------|--------------------------|
| 10 | 56.0 | 1020.6 | 4.3 |
| 9 | 44.4 | 891.9 | 4.1 |
| 8 | 34.3 | 775.6 | 3.9 |

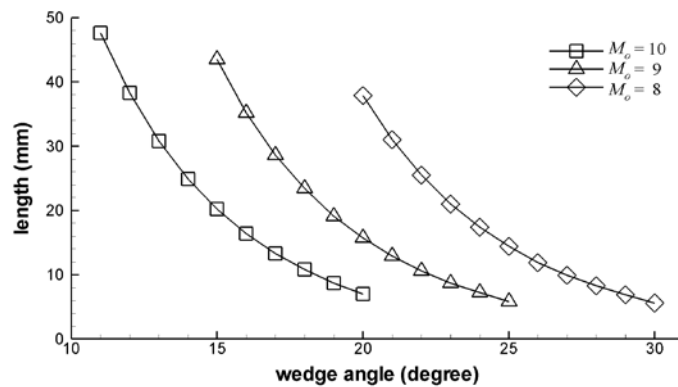


Figure 9 Characteristic length as a function of the wedge angle with flight Mach number M_o of 10, 9, and 8

The numerical results obtained with these parameters for different flight Mach numbers

M_o are shown in Fig. 9. Although the length dependence on wedge angle is similar in the cases of different M_o , it is necessary to adjust the wedge angle to keep the characteristic length on the scale order of several millimeters, which may be an important constraint in the ODWE design. For instance, to obtain the same initiation length with wedge angle of 15° as in the case of flight Mach number $M_o = 10$, the wedge angle should increase to 18.5° and 23° in the cases of $M_o = 9$ and 8 , respectively. Theoretical initiation lengths are also computed for these cases. In the case of $M_o = 9$, error varies from 22.1% to 30.8% when angle changes from 15° to 25° . In the case of flight $M_o = 8$, error varies from 21.5% to 29.9% when angle changes from 20° to 30° . Considering the simple model and assumptions used for the prediction as previously discussed, these errors are acceptable.

IV. Conclusion

In this study, oblique detonation waves in a stoichiometric hydrogen-air mixture are simulated with detailed chemistry. The focus of this paper is given to the initiation process of the oblique detonation wave in practical conditions. In order to mimic the flow in Oblique Detonation Wave Engines (ODWE), the combustible gas mixture with low pressure and high temperature, are derived from practical flight conditions. Under these conditions, numerical results show that the initiation is achieved through the smooth transition from oblique shock to detonation, different from the abrupt transition obtained in previous work. The formation mechanism of the present smooth transition is discussed and the result is found to be consistent with previous theory in literature. Based on the characteristic length of initiation process, quantitative analysis is performed. Results show the initiation length dependence on

the wedge angle and inflow Mach number M_1 is different. Furthermore, it is necessary to increase the wedge angle to keep the characteristic initiation length in a proper range when flight Mach number decreases.

Acknowledgements

The research is supported by NSFC No. 11372333 and 51376165.

References

- [1] K. Kailasanath, "Recent developments in the research on pulse detonation engines," *AIAA J.* **41**, 145-159 (2003).
- [2] A.J. Higgins, "Ram accelerators: outstanding issues and new directions," *J. Propul. Power* **22**, 1170-1187 (2006).
- [3] P. Wokanski, "Detonative propulsion," *Proc. Combust. Inst.* **34(1)**, 125-158 (2013).
- [4] D.T. Pratt, J.W. Humphrey and D.E. Glenn, "Morphology of standing oblique detonation waves," *J. Propul. Power* **7(5)**, 837-845 (1991).
- [5] M.J. Grismer and J.M. Powers, "Numerical predictions of oblique detonation stability boundaries," *Shock Waves* **6**, 147-156 (1996).
- [6] J.M. Powers and K.A. Gonthier, "Reaction zone structure for strong, weak overdriven, and weak underdriven oblique detonations," *Phys. Fluids A* **4(8)**, 2082-2089 (1992).
- [7] J.M. Powers and D.S. Stewart, "Approximate solutions for oblique detonations in the hypersonic limit," *AIAA J.* **30(3)**, 726-736 (1992).

- [8] C.I. Morris, M.R. Kamel and R.K. Hanson, "Shock-induced combustion in high-speed wedge flows," *Proc. Combust. Inst.* **27**, 2157-2164 (1998).
- [9] C. Li, K. Kailasanath, and E.S. Oran, "Detonation structures behind oblique shocks," *Phys. Fluids* **4**, 1600-1611 (1994).
- [10] C. Viguier, L. Figueira da Silva, D. Desbordes and B. Deshaies, "Onset of oblique detonation waves: comparison between experimental and numerical results for hydrogen-air mixtures," *Proc. Combust. Inst.* **26**, 3023-3031 (1996).
- [11] J.P. Sislian, H. Schirmer, R. Dubebout, R. et al., "Propulsive performance of hypersonic oblique detonation wave and shock-induced combustion ramjets", *J. Propul. Power*, **17(3)**, 599-604 (2001).
- [12] G. Fusina, J.P. Sislian and B. Parent, "Formation and stability of near Chapman-Jouguet oblique detonation waves," *AIAA J.* **43(7)**, 1591-1604 (2005).
- [13] M.V. Papalexandris, "A numerical study of wedge-induced detonations," *Combust. Flame* **120**, 526-538 (2000).
- [14] J.Y. Choi, D.W. Kim, I.S. Jeung et al., "Cell-like structure of unstable oblique detonation wave from high-resolution numerical simulation," *Proc. Combust. Inst.* **31**, 2473-2480 (2007).
- [15] H.H. Teng, Z.L. Jiang and H.D. Ng, "Numerical study on unstable surfaces of oblique detonations," *J. Fluid Mech.* **744**, 111-128 (2014).
- [16] H.H. Teng, H.D. Ng, K. Li et al., "Cellular structure evolution on oblique detonation surfaces," *Combust. Flame* **162**, 470-477 (2015).
- [17] M.Y. Gui, B.C. Fan and G. Dong, "Periodic oscillation and fine structure of

- wedge-induced oblique detonation waves,” *Acta Mech. Sin.* **27**, 922-928 (2011).
- [18] J. Verreault, A.J. Higgins and R.A. Stowe “Formation of transverse waves in oblique detonations,” *Proc. Combust. Inst.* **34**, 1913-1920 (2013)
- [19] P.G. Harris, R. Farinaccio, R.A. Stowe et al., “Structure of conical oblique detonation waves,” AIAA paper 2008-4687, 44th AIAA/ASME/SAE/ASEE Joint Propulsion Conference & Exhibit, Hartford, CT, 21-23 July, 2008
- [20] J. Verreault, A.J. Higgins, and R.A., Stowe, “Formation and Structure of Steady oblique and Conical Detonation Waves,” *AIAA J.* **50(8)**, 1766-1772 (2012).
- [21] S. Maeda, S. Sumiya, J., Kasahara et al., “Initiation and sustaining mechanisms of stabilized oblique detonation waves around projectiles,” *Proc. Combust. Inst.* **34(2)**, 1973-1980 (2013).
- [22] S. Maeda, J. Kasahara and A. Matsuo, “Oblique detonation wave stability around a spherical projectile by a high time resolution optical observation,” *Combust. Flame* **159**, 887-896 (2012).
- [23] L. Figueira da Silva and B. Deshaies, “Stabilization of an oblique detonation wave by a wedge: a parametric numerical study,” *Combust. Flame* **121**, 152-166 (2000).
- [24] A.F. Wang, W. Zhao and Z.L. Jiang, “The criterion of the existence or inexistence of transverse shock wave at wedge supported oblique detonation wave,” *Acta Mech. Sin.* **27**, 311-619 (2011).
- [25] H.H. Teng and Z.L. Jiang, “On the transition pattern of the oblique detonation structure,” *J. Fluid Mech.* **713**, 659-669 (2012).
- [26] J.Y. Choi, E.J.R. Shin and I.S. Jeung, “Unstable combustion induced by oblique shock

- waves at the non-attaching condition of the oblique detonation wave,” Proc. Combust. Inst. **32**, 2387-2396 (2009).
- [27] H.H. Teng, Y. Zhang and Z. Jiang, “Numerical investigation on the induction zone structure of the oblique detonation waves,” Comput. Fluids **95**, 127-131 (2014).
- [28] B. Zhang, V. Kamenskihs and H.D. Ng, “Direct blast initiation of spherical gaseous detonations in highly argon diluted mixtures,” Proc. Combust. Inst. **33(2)**, 2265-2271 (2011).
- [29] B. Zhang, H.D. Ng and J.H.S. Lee, “The critical tube diameter and critical energy for direct initiation of detonation in $C_2H_2/N_2O/Ar$ mixtures,” Combust. Flame **159(9)**, 2944-2953 (2012).
- [30] B. Zhang, N. Mehrjoo, H.D. Ng et al., “On the dynamic detonation parameters in acetylene-oxygen mixtures with varying amount of argon dilution,” Combust. Flame **161(5)**, 1390-1397 (2014).
- [31] R. Dubebout, J.P. Sislian, R. Oppitz, “Numerical simulation of hypersonic shock-induced combustion ramjets,” J. Propul. Power, **14(6)**, 869-879 (1998).
- [32] C. Li, K. Kailasanath and E.S. Oran, “Effects of boundary layers on oblique detonation structures,” AIAA paper 93-0450, 31st Aerospace Sciences Meeting & Exhibit, Reno, NV, Jan. 11-14, 1993.
- [33] M. Sun and K. Takayama, “Conservative smoothing on an adaptive quadrilateral grid,” J. Comput. Phys. **150**, 143-180 (1999).
- [34] E.F. Toro, Riemann solvers and numerical methods for fluid dynamics, 2nd ed (Springer, Berlin, 1999).

- [35] R.J. Kee, F.M. Rupley, E. Meeks et al., “Chemkin-II: A Fortran chemical kinetics package for the analysis of gas-phase chemical and plasma kinetics,” UC-405, SAND96-8216, Sandia National Laboratories, 1996.
- [36] P.N. Brown, G.D. Byrne and A.C. Hindmarsh, “VODE, A variable-coefficient ODE solver,” SIAM J. Sci. Stat. Comput. **10**, 1038 -1051 (1989).
- [37] J.H.S. Lee, The detonation phenomenon (Cambridge University Press, New York, 2008).
- [38] Y. Liu, D. Wu, S. Yao, and J. Wang, “Analytical and numerical investigations of wedge-induced oblique detonation waves at low inflow mach number,” Combust. Sci. Technol. **197**, 843-856 (2015).